International Journal of Engineering Research & Technology (IJERT)
ISSN: 2278-0181
Vol. 15 Issue 09 , September - 2026

Improving Single Point GNSS Positioning Accuracy in Canyon Areas by using Virtual Measurements

Prof.Dr. A.K.Abomariam, Dr. R.M.Ali
Civil Engineering Department
Faculty of Engineering El-Mataria
Helwan University
Cairo, Egypt

Eng.A.A.Z.Darwish
M.SC. in Surveying and Geodesy
Faculty of Engineering
Ain Shams University
Cairo, Egypt

Abstract*- Global Navigation Satellite System (GNSS) positioning in urban canyon and other signal-obstructed environments is significantly degraded by signal blockage, satellite masking, and the limited availability of visible satellites. These factors can substantially deteriorate positioning accuracy and, in severe cases, prevent the reliable determination of a position solution. This study proposes an approach based on a Virtual Range Measurement (VRM) to enhance the accuracy and availability of Single Point Positioning (SPP) in challenging urban canyon environments. The proposed approach generates virtual GNSS pseudo-range measurements for satellites that are temporarily blocked or whose observations are considered unreliable. Particular attention is given to the impact of dynamic obstructions, such as large trucks passing in close proximity to a static GNSS receiver, or disappearing a satellite behind stationary obstructions for a certain period, thereby causing temporary signal blockage and degradation. The proposed methodology is developed for static-mode SPP based on code observations, in which the receiver remains stationary and the resulting position estimates are subsequently averaged. The generated virtual measurements are incorporated into the conventional SPP observation model and processed using a weighted least-squares estimation procedure. The performance of the proposed approach is evaluated using GNSS observation data collected under conditions representative of urban canyon environments and is compared with conventional SPP based exclusively on the available real observations. The results indicate that the appropriate integration of virtual measurements can improve satellite geometry, increase the number of effective observations, mitigate measurement noise, reduce positioning errors, shorten the convergence time, and improve the accuracy and stability of the averaged static position without requiring additional physical GNSS infrastructure.

Keywords— SPGNSS, GNSS in canyons, virtual measurements, VRM, Poor DOP, GNSS Non-availability, Static PPP, signal blockage, satellite masking.

I. INTRODUCTION

Global Navigation Satellite Systems (GNSS) have become one of the most important technologies for positioning, navigation, and timing applications. GNSS-based positioning is widely used in surveying, transportation, mapping, intelligent transportation systems, and location-based services because it provides globally referenced position information without requiring local infrastructure. Under open-sky conditions, sufficient satellite availability and favorable satellite geometry (good DOP) generally allow standalone GNSS receivers to provide submeter-level positioning accuracy. However, this performance can deteriorate substantially in environments where the satellite signals are obstructed or severely affected by the surrounding stationary and dynamic objects. [1], [8], [9].

GNSS positioning depends on trilateration concept, where distances from the user to the satellites are measured simultaneously. GNSS positioning needs observations to at least six satellites in case using the three constellations GPS, GLONASS, and GALLIEO to solve the three position parameters, the receiver clock error, and the two intersystem-biases of the constellations [2]. Increasing the number of satellites improves the positioning accuracy and DOP values. On the other hand, there are many error sources when dealing with GNSS observables. These errors are resulting from satellite clock, ionosphere, troposphere, multipath, satellite orbit error, receiver noise, signal blockage, or satellite non-availability, etc. [1], [2], [10].

Numerous GNSS positioning techniques have been developed to mitigate the effects of different error sources and enhance positioning accuracy. Common techniques used in surveying applications include relative and differential positioning, static and kinematic positioning, Real-Time Kinematic (RTK), Virtual Reference Station (VRS), and Precise Point Positioning (PPP). Although these techniques can significantly reduce several GNSS error sources, they cannot completely overcome the loss of satellite observations caused by signal blockage or masking. In particular, when satellites are obstructed by surrounding buildings, terrain, or other high structures, the number of available observations can decrease considerably. This reduction in satellite availability may result in poor satellite geometry, higher Dilution of Precision (DOP) values, reduced observation redundancy, and consequently degraded positioning accuracy, especially in canyon-like environments [2], [9]. Therefore, satellite signal blockage and the resulting loss of GNSS observations remain important challenges that require further investigation and the development of alternative approaches to maintain reliable positioning under severe signal obstruction.

Precise Point Positioning (PPP) is one of the most important observation modes for high-precision surveying when differenced observations are not available because the receiver remains stationary at the point of interest while continuously collecting observations over an extended period. The extended observation period provides a larger number of redundant measurements from different satellite geometries, allowing random errors and short-term variations in the observations to be reduced through statistical processing. Consequently, static PPP surveying is widely regarded as a fundamental technique

International Journal of Engineering Research & Technology (IJERT)
ISSN: 2278-0181
Vol. 15 Issue 09 , September - 2026

for low-cost mapping applications [1], [2], [10]. In this context, the lost measurements from the blocked or masked satellites during the observation session will negatively affect the final averaged results.

The virtual satellite signal generation is one of the strategies used for solving the satellites unavailability problem [3]. It may be defined as the process of generating simulated GNSS signals that mimic the signals transmitted by real GNSS satellites. This strategy has many advantages which are as follows: non-line of sight is required between the receiver and satellite, increasing the redundant measurements, and in turn improving the DOP values and positioning accuracy. The satellite signal that is to be easily generated is the code signal represented by the Pseudo-Range measurement. It represents the measured distance between the satellite and the receiver [4].

There are many previous studies were trying to improve the GNSS positioning and DOP values by using the virtual satellites and measurements. These previous trials took some assumptions in its algorithms like: putting a constant virtual satellite at distant virtual position depending upon supposed good DOP [3], [4], maintaining the satellite clock error and altitude of the receiver just entering the canyon areas, using extra radio hardware [5] and maintaining the differential error obtained from last good geometric distribution for the satellites before entering the harsh areas [6]. In this context, the previous studies did not use the updated corrections and satellites real positions at each epoch inside the canyon areas.

On the other hand, the current paper uses the precise ephemerids to get the satellite real positions of the lost and visible satellites besides the real corrections at each epoch inside the canyon areas. In this way, a new algorithm is proposed to generate VRM for the lost satellites to improve the positioning accuracy and DOP. Besides, a new software is developed based on this new algorithm. Applying this new algorithm to a case study in Egypt, the results are to be compared to those obtained by the traditional solution.

II. GENERATING THE VIRTUAL PSEUDORANGE MEASUREMENT (VRM)

The VRM is generated by adding the errors to the geometrical distance between the receiver and the lost satellite as in (1), where VRi and GDi are the virtual range and the geometrical distance for the lost satellite i respectively, Ei is the total range error that may be modeled for satellite i. The receiver position is obtained here as an approximate from the last sufficient visible satellites before signal cut-off. In this context, the algorithm will remain the good DOP along through the solution when poor DOP is encountered. The satellite position is obtained from the precise ephemerides sp3 file downloaded via the IGS website [7]. Equation (2) presents the geometrical distance between the receiver and the GNSS satellite, where (xi,yi,zi) and (xr,yr,zr) are the Cartesian coordinates of the satellite i and the receiver respectively.

$$VR_i = GD_i + E_i \tag{1}$$

$$GD_i = \sqrt{(x_i - x_r)^2 + (y_i - y_r)^2 + (z_i - z_r)^2} \tag{2}$$

Here, Ei represents the total error that may exist in the range measured from the satellite to the receiver including the ionosphere, troposphere, satellite clock, receiver clock, orbit, and other errors. Note here that, the measurement noise and multipath error are not considered in the virtual range measurement and is considered only in the actual measurements for the visible satellites. Accordingly, it is expected that the multipath effect and noise will be reduced somewhat in this algorithm. The multipath effect of the visible satellites may be reduced by using receivers with special filters and technology [2]. In SPGNSS technique, the receiver clock errors and intersystem biases are considered as additional parameters in the solution, the ionospheric error can be removed by using the ionospheric free model, the tropospheric error can be computed by the Saastamoinen model [1], [2]. Both the precise positions and clock corrections of the satellites may be got from the precise files on the IGS web sites [7]. In our case, some of the satellites are lost whom their measurements are virtual. For simplicity, Figure (1) shows only two satellites one is visible and the other is lost. SV1 and SL1 are the visible and lost satellites respectively. P1V1 and P2V1 are the pseudo ranges from the receiver unit to the visible satellite on the L1 and L2 carriers respectively. VR1L1 and VR2L1 are the virtual ranges from the receiver to the lost satellite on the L1 and L2 carriers respectively.

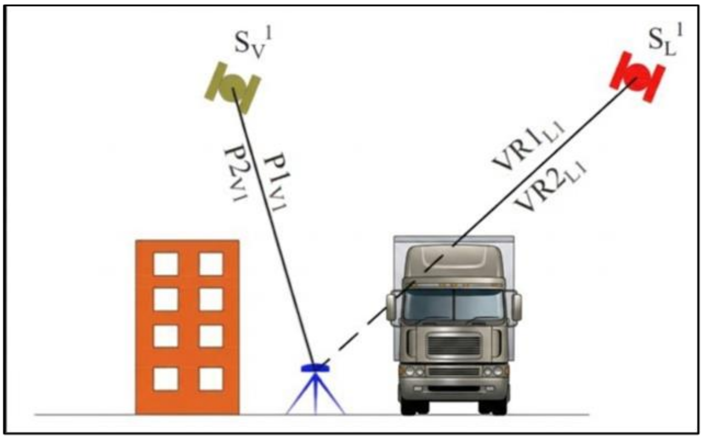

Fig. 1. visible and lost satellites in canyon areas

The ionospheric-free models of these real and virtual ranges can be presented in (3) and (4) respectively, where GD, T, δT, δt, ISB, M, and ε are the geometric distances, tropospheric error, satellite clock error, receiver clock error, inter-system bias, multipath effect, and noise respectively, taking into account the appropriate subscripts of the satellites. The subscripts definition are as follows: Vi, Li are for the visible and lost satellite i respectively. The abbreviations f1 and f2 are the frequencies of the two carriers L1 and L2 respectively. Multipath and noise can be reduced by the special filters in the receivers. we can deduce that the total error Ei of the lost satellite is represented by (5). Finally, as in (1), the ionospheric-free virtual range, consisting of both the virtual ranges on the L1 and L2 carriers, can be represented by (6).

International Journal of Engineering Research & Technology (IJERT)
ISSN: 2278-0181
Vol. 15 Issue 09 , September - 2026

$$P_{IF} = \frac{f_1^2.P1V1-f_2^2P2V1}{f_1^2-f_2^2} = GD_{V1} + T_{V1} + \delta T_{V1} + \delta t + ISB_{V1} + M_{V1} + \varepsilon_{V1} \quad (3)$$

$$V_{IF} = \frac{f_1^2.VR1L1-f_2^2VR2L1}{f_1^2-f_2^2} = GD_{L1} + T_{L1} + \delta T_{L1} + \delta t + ISB_{L1} \quad (4)$$

$$E_i = T_{L1} + \delta T_{L1} + \delta t + ISB_{L1} \quad (5)$$

$$V_{IF} = GD_{L1} + E_i \quad (6)$$

III. SPGNSS POSITIONING NORMAL EQUATIONS SYSTEM

In this paper, the visible and lost satellites should be considered in the SPGNSS positioning normal equations. Equations (3) and (4) represent the observation equations for the visible and lost satellites, respectively, for one epoch. Assuming having NV visible satellites and NL lost satellites, then the number of observation equations is (NL+NV) and the number of unknowns is 6 that is the coordinates of the receiver, the receiver clock error, ISBGLO and ISBGAL as in (7). Note that ISBGLO and ISBGAL are the inter system biases of the GLONASS and GALILEO time systems respectively. These equations can be written in notation matrix as in (8). [A] matrix is the partial derivative of the observation equations w.r.t the unknowns [X], as depicted in (9). $\frac{\partial L_{V1}}{\partial x}$, $\frac{\partial L_{V1}}{\partial y}$, $\frac{\partial L_{V1}}{\partial z}$, $\frac{\partial L_{V1}}{\partial \delta t}$, $\frac{\partial L_{V1}}{\partial ISBGLO}$, and $\frac{\partial L_{V1}}{\partial ISBGAL}$ are the partial derivative of the observation equation for the first visible satellite w.r.t the unknowns respectively. Similarly, $\frac{\partial L_{L1}}{\partial x}$, $\frac{\partial L_{L1}}{\partial y}$, $\frac{\partial L_{L1}}{\partial z}$, $\frac{\partial L_{L1}}{\partial \delta t}$, $\frac{\partial L_{L1}}{\partial ISBGLO}$, and $\frac{\partial L_{L1}}{\partial ISBGAL}$ are those of the first lost satellite. [V] is the residual array. Equation (10) shows [L], the misclosure array, that is the measured minus computed values. The elements of this array can be presented in (11) and (12) as an example for the visible and lost satellites respectively. [P] is the weight matrix composing of the reciprocal sine of the elevation angles of the satellites as indicated in (13) [2], [10]. This system of equations can be solved by the least squares method e.g. [2].

$$X = \begin{bmatrix} X_r \\ Y_r \\ Z_r \\ \delta t \\ ISBGLO \\ ISBGAL \end{bmatrix} \quad (7)$$

$$PAX = PL + V \quad (8)$$

$$A = \begin{bmatrix} \frac{\partial L_{V1}}{\partial x} & \frac{\partial L_{V1}}{\partial y} & \frac{\partial L_{V1}}{\partial z} & \frac{\partial L_{V1}}{\partial \delta t} & \frac{\partial L_{V1}}{\partial ISBGLO} & \frac{\partial L_{V1}}{\partial ISBGAL} \\ & & & \cdots & & \\ & & & \cdots & & \\ \frac{\partial L_{NV}}{\partial x} & \frac{\partial L_{NV}}{\partial y} & \frac{\partial L_{NV}}{\partial z} & \frac{\partial L_{NV}}{\partial \delta t} & \frac{\partial L_{NV}}{\partial ISBGLO} & \frac{\partial L_{NV}}{\partial ISBGLO} \\ \frac{\partial L_{L1}}{\partial x} & \frac{\partial L_{L1}}{\partial y} & \frac{\partial L_{L1}}{\partial z} & \frac{\partial L_{L1}}{\partial \delta t} & \frac{\partial L_{L1}}{\partial ISBGLO} & \frac{\partial L_{L1}}{\partial ISBGAL} \\ & & & \cdots & & \\ & & & \cdots & & \\ \frac{\partial L_{NL}}{\partial x} & \frac{\partial L_{NL}}{\partial y} & \frac{\partial L_{NL}}{\partial z} & \frac{\partial L_{NL}}{\partial \delta t} & \frac{\partial L_{NL}}{\partial ISBGLO} & \frac{\partial L_{NL}}{\partial ISBGAL} \end{bmatrix} \quad (9)$$

$$L = \begin{bmatrix} l_{V1} \\ . \\ . \\ l_{NV} \\ l_{L1} \\ . \\ . \\ l_{NL} \end{bmatrix} \quad (10)$$

$$l_{V1} = GD_{V1} + T_{V1} + \delta T_{V1} + \delta t + ISB_{V1} + M_{V1} + \varepsilon_{V1} \quad (11)$$

$$l_{L1} = GD_{L1} + T_{L1} + \delta T_{L1} + \delta t + ISB_{L1} \quad (12)$$

$$P_i = \frac{1}{\sin(Elevation)} \quad (13)$$

IV. THE GENERAL ALGORITHM

Based on generating the virtual range and the SPGNSS positioning normal equations discussed in sections II and III, a new algorithm is developed for processing the GNSS received data to improve the DOP and the positioning accuracy. The main idea of this algorithm is to simulate the lost satellites and generate a virtual measurement for them in order to increase the number of the positioning equations. In this context, the DOP and positioning accuracy will be improved. Figure (2) shows the process flowchart. The algorithm starts with reading the receiver Rinex file. After analyzing the data, a report about the lost and visible satellites can be presented. Then the SP3 and CLK files, downloaded from the IGS website [7], of the precise ephemerids of the satellites is read to compute the coordinates and clock corrections of them at the observation epochs using Lagrange models [2]. Before losing any of the satellites, an approximate position for the receiver is obtained by the possible visible satellites. Using this approximate position of the receiver and that precise coordinates for the satellites, the virtual ranges for the lost satellites are generated, as discussed in section II. Solving the SPGNSS positioning equations by sequential least squares, as discussed in section III, a new position for the receiver is obtained. This process is iterated till the NOEP (number of epochs).

International Journal of Engineering Research & Technology (IJERT)
ISSN: 2278-0181
Vol. 15 Issue 09 , September - 2026

In order to execute this algorithm practically, a new software is developed by the author using visual basic.net and MATLAB programming languages. The algorithm can be applied on the receiver observation data by running this software and the intended results can be achieved. Figure (3) shows the interface of the developed software. Through this interface, you can select the paths of the input and output files, display the sky and time plots, and process the data.

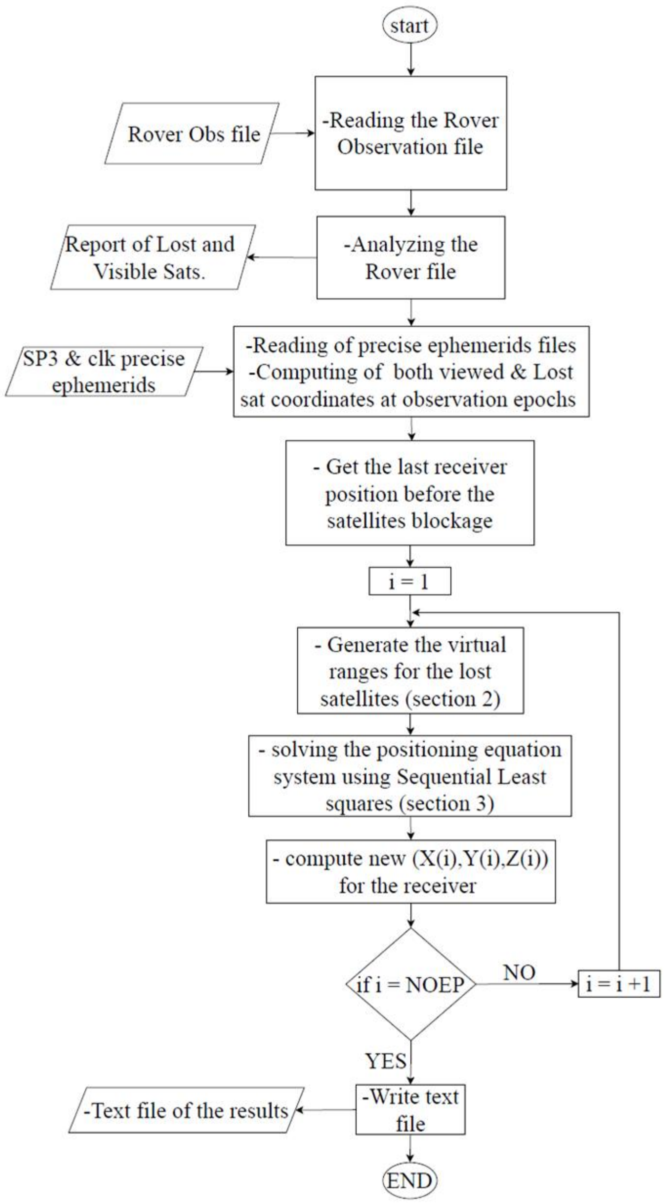

Fig. 2. Flowchart of the algorithm for improving the SPGNSS DOP and positioning accuracy by VRM

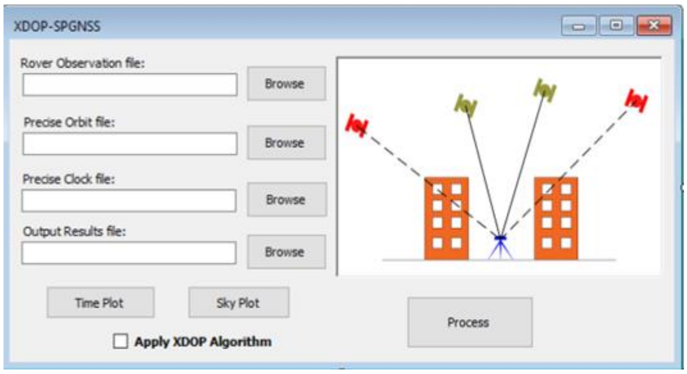

Fig. 3. A new developed software (XDOP-SPGNSS) for improving the DOP and positioning accuracy in case of lost satellites by VRM

V. APPLYING THE ALGORITHM ON REAL OBSERVATION DATA (CASE STUDY)

In this case study, A GNSS (GPS, GLONASS, and GALLILEO) observation data was collected in Cairo-Egypt in the static mode by only single receiver. The observation session is about 30 minutes (1780 seconds), and the observation interval is one second. The Full available satellites in the original case were about 24 GNSS satellites, see Figures (4a) and (4b). Another data file is extracted from the original one that containing only 6 satellites simulating masking of 18 satellites along the observation period. This last data file is processed by both the traditional and proposed techniques. The results are compared with those obtained by the traditional solution of the original full availability satellites and presented in tables and charts. Table (1) shows the statistical parameters like maximum, minimum, range, mean, and standard deviation at both 68% and 95% confidence levels, and the root mean square error. Also, the results of Easting error, Northing error, Height error are layout through Figure (5) to Figure (7). In addition, a graph of the DOP values for the Proposed and Traditional solution is presented in Figure (8). The convergence time for Easting, Northing, and Height are presented through the graphs in Figure (9) to Figure (11).

An analysis of the empirical results presented in the tables and figures demonstrates a significant enhancement in absolute positioning accuracy when utilizing the proposed algorithm. This optimization is evident across both horizontal and vertical components, as quantified by the reduction in the respective mean error values. Notably, the substantial contraction in the error bounds and standard deviation metrics indicates that the proposed framework achieves superior smoothing capabilities, effectively suppressing high-frequency measurement noise and multipath effects inherent in standard processing.

Furthermore, the geometric strength of the solution is considerably strengthened, as substantiated by the improved Position Dilution of Precision (PDOP) profiles illustrated in Figure (8). In terms of temporal efficiency, the proposed algorithm exhibits an accelerated convergence profile relative to traditional processing strategies. Crucially, the initialization period required to attain steady-state, sub-meter precision is markedly shortened, validating the efficiency of the new methodology for time-critical geodetic applications.

International Journal of Engineering Research & Technology (IJERT)
ISSN: 2278-0181
Vol. 15 Issue 09 , September - 2026

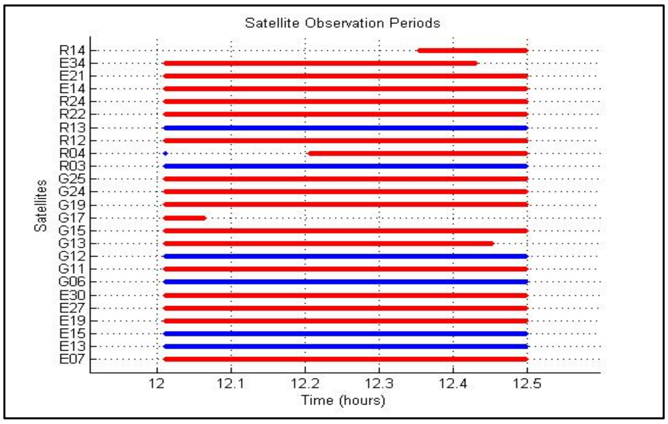

Fig. 4a. Time-Plot for the satellites of the case study in Cairo. Visible and lost satellites are indicated by blue and red colors respectively.

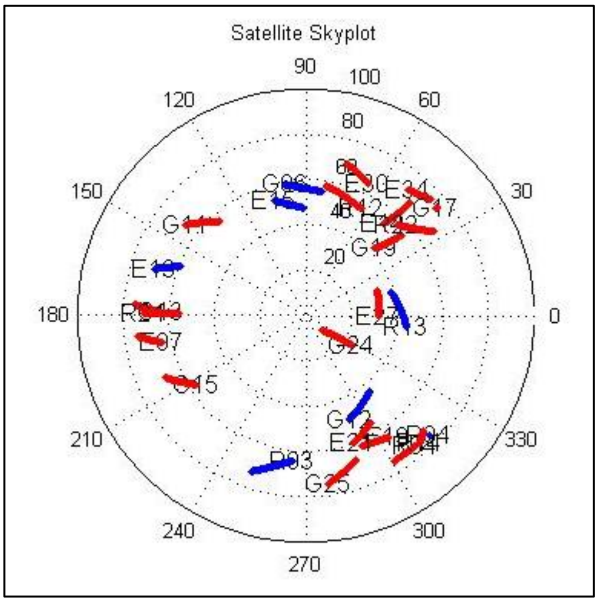

Fig. 4b. Sky plot for the satellites of the case study in Cairo. Visible and lost satellites are indicated by blue and red colors respectively.

Table 1. comparison between the positioning errors obtained from the traditional and proposal solution

	Traditional Solution			**Proposal Solution**		
	E (m)	**N (m)**	**H (m)**	**E (m)**	**N (m)**	**H (m)**
Max.	-3.176	18.485	30.655	0.265	2.987	10.195
Min.	-5.292	-1.606	-30.784	-1.638	-2.281	-7.844
Range	2.116	20.091	61.439	1.903	5.268	18.039
Mean	-4.041	7.583	0.595	-0.634	1.031	1.060
1σ (68%)	0.367	3.099	8.625	0.283	0.664	2.478
2σ (95%)	0.716	6.042	16.818	0.552	1.296	4.832
RMSE	4.060	8.195	8.645	0.695	1.227	2.696

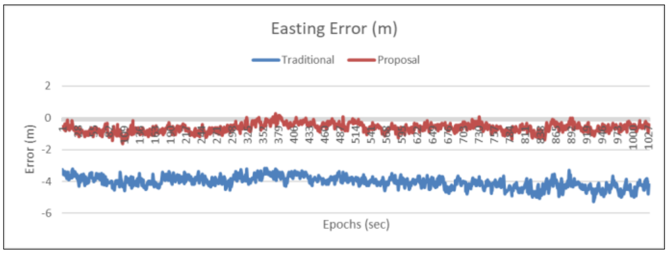

Fig. 5. Comparison between the traditional and proposed solutions in the Easting direction

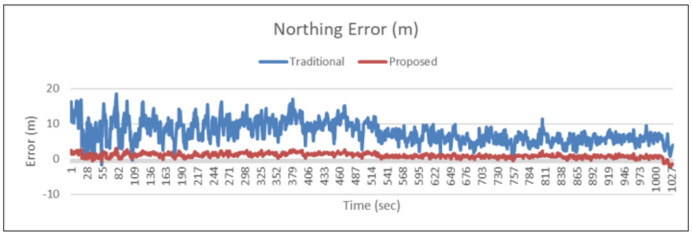

Fig. 6. Comparison between the traditional and proposed solutions in the Northing direction

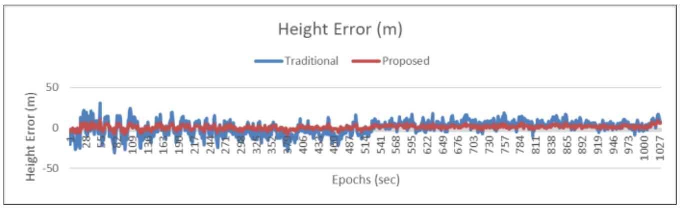

Fig. 7. Comparison between the traditional and proposed solutions in the Elevation direction in Alex case

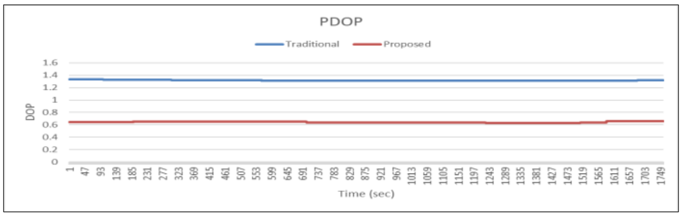

Fig. 8. Comparison between the traditional and proposed solutions in the PDOP values

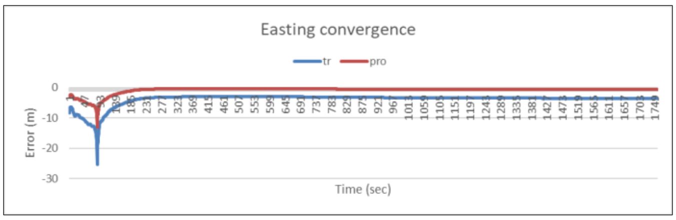

Fig. 9. Comparison for the convergence time between the traditional and proposed solutions in the Easting direction

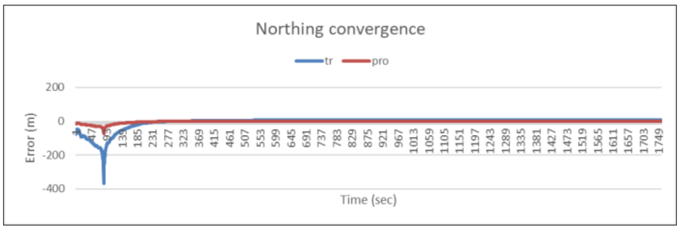

Fig. 10. Comparison for the convergence time between the traditional and proposed solutions in the Northing direction

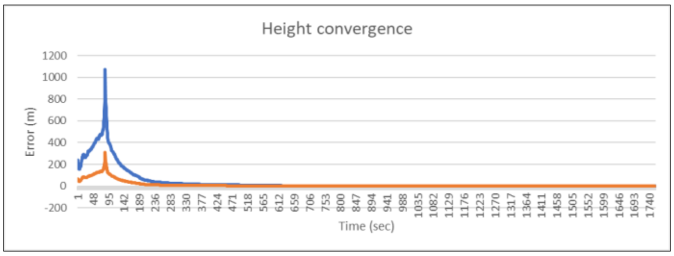

Fig. 11. Comparison for the convergence time between the traditional and proposed solutions in the Height direction

VI. CONCLUSIONS

Based on the preceding empirical evaluations and theoretical discussions, the primary findings of this research are summarized as follows:

- **Algorithmic Innovation for Urban Canyons:** A novel processing framework has been successfully developed to enhance absolute positioning performance in constrained environments. The methodology improves geometry and positioning precision by synthesizing virtual pseudo-range measurements to supplement signals from physically obstructed or masked satellites during single-point static sessions.
- **Software Implementation:** To validate this methodology, a specialized software utility was engineered to execute the core mathematical model, ingest raw GNSS observation files, and compute optimized position solutions. The software was rigorously evaluated using representative empirical case studies. Using this new algorithm for the case study in this paper, if only 6 GNSS satellites are visible, the positioning noise and accuracy results represented by the error range, standard deviation, mean and PDOP are reasonably smoothed and improved. The great improvement in the error range and standard deviation values indicates that great smoothing is achieved in the noise of the proposed solution.
- **Noise Mitigation and Geometric Optimization:** Empirical testing under constrained conditions (e.g., configurations with only six physically visible satellites) demonstrates substantial improvements across all key performance metrics. The proposed algorithm significantly reduces the Position Dilution of Precision (PDOP) and minimizes mean positioning errors. Most notably, the pronounced contraction in both the overall error range and the standard deviation values confirms that the algorithm successfully mitigates high-frequency receiver noise and site-specific multipath effects.
- **Temporal Efficiency:** The initialization profile of the position solution exhibits marked acceleration, with the overall convergence time required to achieve steady-state accuracy being substantially shortened compared to traditional single-point processing.

VII. RECOMMENDATIONS

According the preceding results and conclusions, the following recommendations are suggested:

- This paper concentrates on the single point GNSS static mode, it is recommended to modify the algorithm to be able for solving the kinematic data with the help of (IMU) Inertial Movement Unit.
- This research may be a base for other investigations in which a more robust algorithm is composed taking into considerations a more reliable technique for multipath mitigation and cycle clips and other errors.

REFERENCES

[1] El-Rabbany, “Introduction to the Global Positioning System (GPS)”. Artech House Mobile Communication Series, Boston, London, 2002.

[2] B. Hofmann-Wellenhof, H. Lichtenegger, and E. Wasle, Global Navigation Satellite Systems: GPS, GLONASS, Galileo, and More. Vienna, Austria: Springer, 2008.

[3] I.-T. Kim, C. S. Park, G.-I. Jee, and J. G. Lee, “GPS positioning using virtual pseudorange,” Control Engineering Practice, vol. 6, no. 1, pp. 25–35, Jan. 1998, doi: 10.1016/S0967-0661(97)10060-0.

[4] C. Song, J. Ahn, M. Choi, J. Jang, M. Heo, and Y. Lee, “Virtual satellite and virtual range measurement generation for the GNSS position accuracy improvement,” Journal of the Korean Society for Aeronautical & Space Sciences, vol. 45, no. 9, pp. 757–765, 2017, doi:10.5139/jksas.2017.45.9.757

[5] M. Femminella and G. Reali, “Low Satellite Visibility Areas: Extension of the GPS Capabilities to Deploy Location-Based Services,” IEEE Vehicular Technology Magazine, vol. 7, no. 4, pp. 55–65, 2012.

[6] J. H. Bong, D. Kim, and S. Jeong, “GNSS performance enhancement using measurement estimation in harsh environment,” PLoS One, vol. 18, no. 9, p. e0292116, 2023, doi: 10.1371/journal.pone.0292116.

[7] International GNSS Service, “Home – IGS,” https://igs.org/

[8] Misra, P., & Enge, P. (2011). Global Positioning System: Signals, Measurements, and Performance (2nd ed.). Ganga-Jamuna Press.

[9] Kaplan, E. D., & Hegarty, C. J. (Eds.). (2017). Understanding GPS/GNSS: Principles and Applications (3rd ed.). Artech House.

[10] Abdel-Salam, M. A. (2005). Precise point positioning using un-differenced code and carrier phase observations (UCGE Report No. 20229) [Doctoral dissertation, University of Calgary, Department of Geomatics Engineering]. University of Calgary